Properties of elastic percolating networks in isotropic media with arbitrary elastic constants

O. Pla
Instituto de Ciencia de Materiales, Consejo Superior de Investigaciones Científicas, Facultad de Ciencias, Universidad Autónoma, E-28049 Madrid, Spain

R. Garcia-Molina
Departamento de Física Aplicada, Facultad de Ciencias, Universidad de Murcia, E-30071 Murcia, Spain

F. Guinea
Instituto de Ciencia de Materiales, Consejo Superior de Investigaciones Científicas, Facultad de Ciencias, Universidad Autónoma, E-28049 Madrid, Spain

E. Louis
Departamento de Física Aplicada, Facultad de Ciencias, Universidad de Alicante, Apartado 99, E-03080 Alicante, Spain

(Received 22 November 1989)

The properties of diluted elastic media in two dimensions are investigated in an isotropic system in which the ratio between the two Lamé coefficients can be varied. Changes in the ratio between the continuum elastic constants induce significant variations in the behavior of the system away from the threshold for percolation, but not in the properties near the percolation transition. We discuss the results in both cases and their relevance to the definition of the universal properties of diluted elastic networks. It is shown that many features of interest, like the bulk modulus at intermediate concentrations of voids and the backbone, are very dependent on the microscopic details of the model, and not only on its macroscopic behavior. Thus, elastic percolation does not seem to have the same degree of universality as scalar percolation.

I. INTRODUCTION

Most of the existing literature on elastic percolation[1-4] supports the widely accepted view that the critical properties of the percolation transition are independent of the macroscopic properties of the system (elastic moduli), being solely determined by the topology of the medium, as in the case of scalar percolation.[5] The latter can be changed by varying either the underlying lattice or the interactions within it. Although the dependence on the lattice of the critical properties seems well founded, it has recently been claimed that a more general type of universality exists and that the critical exponents are not only independent of the elastic constants of the system but also of the nature of the microscopic interactions.[6]

The possibility that the critical properties of an elastic network are independent of the initial (macroscopic) elastic moduli has been investigated by the present authors, for an isotropic elastic medium with arbitrary elastic constants.[7,8] The elastic system is described by a central-force Hamiltonian in a triangular lattice. Two different force constants are used, to allow variations of the ratio of the Lamé coefficients,[9] which are calculated taking the continuum limit of the discrete equations. Although in that work it was concluded, from the numerical results, that both the percolation threshold and the critical exponents varied with the elastic constants, recent analysis of that system indicates that at least the percolation threshold does not depend on the elastic constants;[8] its value remains equal to that of the unreconstructed triangular lattice.[6,10] The purpose of this paper is to present a thorough investigation of the model introduced in Ref. 7. It turns out that the system shows a behavior far more intricate than could be anticipated, adding a possible new source of nonuniversality in elastic percolation problems to those indicated previously.

The rest of the paper is organized as follows: in Sec. II we describe the model and indicate the relationship between the ratio of Lamé coefficients and the ratio of the two force constants used in the discrete Hamiltonian. Next (Sec. III) we discuss the most relevant features of the numerical methods used to solve the equilibrium equations of the diluted network. The properties of diluted networks are analyzed next (Sec. IV), as well as various test cases used to facilitate the understanding of the results. An extension of effective medium theories successfully used to describe the simple triangular lattice[4,11,12] is also presented. The way the bulk and shear moduli approach zero is analyzed, as well as the main features of the backbone, which gives rigidity to the structure slightly above p_{cen}. The main conclusions comprise the last section of the paper.

II. THE MODEL

We describe the elastic energy of the system by means of the rotationally invariant central force Hamiltonian:

$$H = \frac{1}{2}\sum_{i,j} k_{ij}[(\mathbf{v}_i - \mathbf{v}_j)\cdot \hat{\mathbf{r}}_{ij}]^2, \tag{1}$$

where $\hat{\mathbf{r}}_{ij}$ is a unit vector between sites i and j. The force constants, k_{ij}, are finite with probability p and zero otherwise. $\mathbf{v}_i$ is the displacement vector at site i.

As the only bidimensional regular lattice that gives the isotropic continuum limit[9] is the triangular one, Eq. (1) is imposed in that lattice. The ratio of the two Lamé coefficients is adjusted by using two different values for the force constants (k_a and k_b), that is, two types of springs. They are distributed over the lattice in the manner depicted in Fig. 1. The unit cell is three times larger than that of a simple triangular lattice, giving rise to a $\sqrt{3}\times\sqrt{3}$ reconstruction.

We find the relation between the Lamé coefficients and the force constants of the discrete model by calculating the density of the elastic energy under hydrostatic compression and shear, both for the lattice and the continuum model. In the latter case, the energy density is given by[9]

$$E_c = \frac{\lambda_0}{2}(u_{xx}+u_{yy})^2 + \mu_0(u_{xx}^2 + u_{xy}^2 + u_{yx}^2 + u_{yy}^2), \tag{2}$$

where $u_{ij}(i,j = x,y)$ are the components of the strain tensor, and λ_0 and μ_0 are the Lamé coefficients. Then, in order to calculate the bulk $B_0 = \lambda_0 + \mu_0$ and shear μ_0 moduli, we introduce displacements at the boundaries so as to induce a uniform dilation or a pure shear distortion. In the latter case, special care is required to ensure that all the nodes in the reconstructed lattice are at equilibrium. Let us call δ the magnitude of the strain field. In the continuum limit we have

$$E_c = \begin{cases} 2(\lambda_0+\mu_0)\delta^2 & \text{(3a)} \\ \frac{2}{3}\mu_0\delta^2, & \text{(3b)} \end{cases}$$

for dilation and shear, respectively, whereas in the discrete case, the elastic energy per bond is given by

$$E_d = \begin{cases} \dfrac{2k_b + k_a}{6}\delta^2 & \text{(4a)} \\ \dfrac{k_a k_b}{4(k_b+2k_a)}\delta^2, & \text{(4b)} \end{cases}$$

for dilation and shear, respectively; thus, by equating the ratio between the energy densities for shear and compression in the two cases, we find[13]

$$\frac{\lambda_0}{\mu_0} = \frac{4x^2+x+4}{9x}, \quad x = \frac{k_a}{k_b}. \tag{5}$$

The ratio λ_0/μ_0 does not vary when k_a and k_b are exchanged. Notice also that the shear modulus vanishes when either k_a or k_b tend to zero. This behavior is easily understood by noting that when $k_a = 0$ the remaining bonds lie in a honeycomb lattice, which has no shear in the central-force model, whereas, for $k_b = 0$, the morphology of the bond structure is isomorphic to the square lattice, for which also $\mu_0 = 0$ within that model.

The model allows us to vary λ_0/μ_0 continuously between 1 and infinity, and it is, therefore, well suited to study the properties of elastic media whose macroscopic moduli lie in a rather wide range. The discrete system, however, is different from the combination of bond-bending and bond-stretching forces more commonly used in the literature to derive media with arbitrary elastic constants.[2]

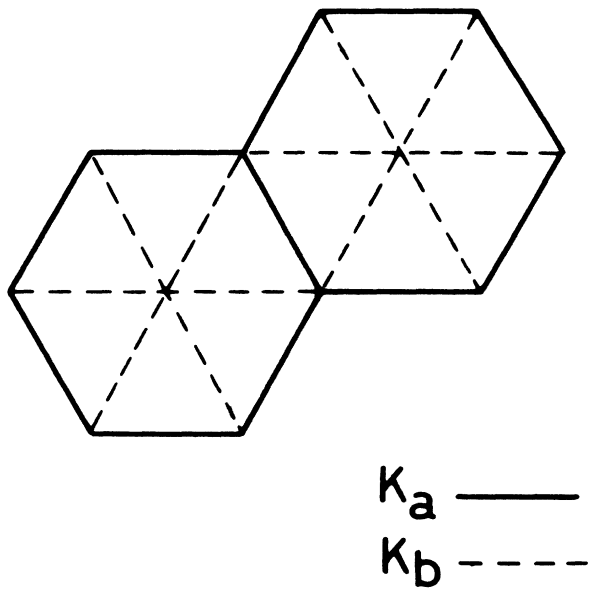

FIG. 1. The $\sqrt{3}\times\sqrt{3}$ reconstruction of the triangular lattice utilized in this work.

III. NUMERICAL METHODS

The crucial importance of the accuracy of the numerical procedures used to investigate the properties of diluted networks near the percolation threshold is widely accepted. Two types of methods can be clearly differentiated. In the first place we mention those methods that use finite samples of arbitrary shape, and we solve the equilibrium equations by means of a given iterative procedure[14] (i.e., letting the system go towards equilibrium step by step). The second class of methods is based upon the transfer-matrix approach[10] first applied to the scalar percolation problem; in this case the samples are long strips of varying width. The most important shortcoming of these later methods is that they do not keep the information of the spatial distribution of stresses and are therefore not suited to studying the properties of the backbone; on the other hand, they seem to be most pow-

erful in investigating the critical properties at the percolation threshold. The first group of methods seems to be less accurate than the second one in calculating the critical exponents and percolation threshold, although they are commonly used to study the stress distribution of the backbone.

In this work we use finite hexagonal samples of the triangular network, characterized by the length of the side of the hexagon L, expressed in units of the distance between nearest neighbors. The boundary conditions (dilation or shear) are imposed by fixing the displacements of the nodes at the border of the hexagon, which implies the corresponding rearrangement of all the internal nodes in order to keep the system in equilibrium. The use of a dilation boundary condition is done to preserve the isotropy of the system. Other works use uniaxial boundary conditions, in particular those that use the transfer-matrix method. This can have some implications in the size dependence of the problem, but not in the numerical method used (transfer-matrix and iterative methods should give the same size dependence provided that boundary conditions are the same).

After removing a fraction $1-p$ of the bonds of the sample [each sample has $3L(3L-1)$ bonds that can be removed], the equilibrium equations are to be solved. We have tried two iterative methods of solving these equations: the conjugate gradient method (CGM) and the relaxation method (RM). The appropriateness of both methods has been checked in two ways: the first and more simple one is to look at how much stress each node accumulates, and the result is that, after a small number of iterations, CGM shows better precision. Another way of checking numerical methods is to look at the distribution of stresses once the diluted network is relaxed. In this distribution, and for the case $\lambda_0/\mu_0 = 1$ (triangular unreconstructed lattice), two peaks are found (see the following): one placed at a stress that is almost independent of the accuracy of the method and that corresponds with the backbone that supports elastic energy, and another peak, formed by unstressed bonds, that should be located at zero stress, but, because of numerical accuracy, stays at a finite value. When solving the equilibrium equations by means of RM, these two peaks are merged into a broader one even after a huge number of iterations (the number of bonds that contribute to the stiffness of the network is increased only by numerical errors), whereas for CGM a clear two-peak feature is observed even for relatively large values of the CGM error. Moreover, the soft-mode's peak can be displaced by varying this CGM error, so it can be a means to fix a minimum error that will allow a confident savings of computer time. The numerical calculations for percolation samples presented in this work were performed by CGM with a maximum allowed error of 10^{-9} (CGM standard error). Hexagonal samples of sides in the range 6–48 (in units of bond length) were considered, the number of realizations for each size being in the range 10–200 (the higher the number, the smaller the size). The number of CGM iterations needed to achieve the convergence was found to increase with the size of the sample and with the k_a/k_b ratio. The investigation of the properties of the backbone was carried out on samples of size 30 (around ten realizations were considered). The CGM error was fixed at 10^{-12}, which corresponds on average to a maximum force on the nodes 10^{-7} times the displacement on the boundary nodes. The number of iterations required to achieve this accuracy was found to depend strongly on p and k_a/k_b. For instance, for $k_a/k_b = 1$, between 400 and 700 iterations were required for p far from the threshold; instead, at $p = 0.65$ the fixed accuracy was obtained only after 5000–10 000 iterations. For $k_a/k_b = 0.05$, the number of iterations had to be increased by a factor of 3; those realizations for which the desired accuracy was not attained after 30 000 iterations were not included in the analysis of the stress distribution.

IV. ELASTIC PROPERTIES OF DILUTED NETWORKS

A. Hexagonal rings

We first discuss the results obtained for a small concentration of broken bonds, far from the percolation threshold. These results show a pronounced dependence on the ratio λ_0/μ_0, and also on the way in which this value is obtained, that is, the choice of discrete lattice (notice that λ_0/μ_0 is invariant under an exchange of k_a and k_b). Hence, we think that they are relevant to the question of which properties of elastic percolation are genuinely universal and which ones depend on the microscopic details of the model and cannot be easily generalized.

As a first check that our lattice describes the continuum elasticity equations at large scales well, we have analyzed the elastic moduli of hexagonal samples from which a smaller hexagon has been removed from the center. This situation is well approximated, in the continuum limit, by a ring under applied pressure. Then, the bulk modulus B varies as a function of the relative size of the internal void as[7]

$$B = \frac{B_0 p}{1 + (1 + \lambda_0/\mu_0)(1-p)}, \tag{6}$$

where B_0 is the bulk modulus when $p = 1$. Numerical results and analytical curves obtained from (6) are shown in Fig. 2. There is a good agreement for very different values of λ_0/μ_0, which indicates that the model correctly reproduces the continuum limit.

The results presented are relevant to the percolation problem, when the concentration of broken bonds is small. Then the system can be regarded as containing a few small cracks, which independently influence the macroscopic elastic constants. Effects associated with the interaction between voids are proportional to the square of the concentration of voids. Each of these voids gives an additive contribution to the softening of the sys-

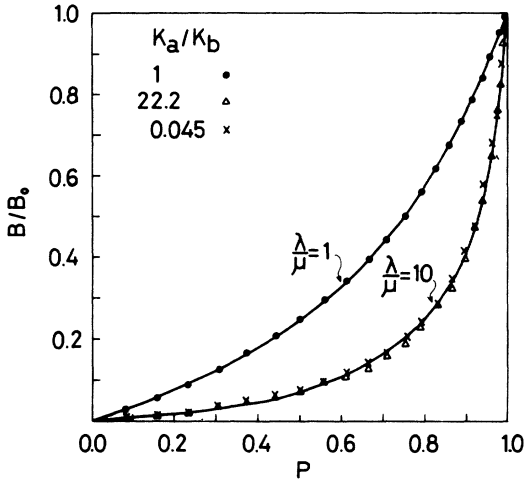

FIG. 2. Bulk modulus vs p for circular rings of the continuous isotropic media (continuous lines) and hexagonal rings of the reconstructed triangular lattice (discrete values) as given by Eq. (6) and numerical calculations, respectively.

tem, and the overall change can be obtained from (6) by linearizing around $p = 1$:

$$\frac{B}{B_0} = 1 - (1-p)\left(2 + \frac{\lambda_0}{\mu_0}\right). \tag{7}$$

Thus, the decrease of B is enhanced by a large value of λ_0/μ_0. This trend is present in the results obtained using a discrete lattice, although, as will be discussed, there are also modifications that not only depend on λ_0/μ_0 but also on the way in which the continuum limit is implemented in the discrete lattice.

B. Random voids: Effective medium theory and numerical results

We can proceed further analytically by extending the effective medium theory developed in Refs. 4, 11, 12, and 15. In order to generalize it to our reconstructed lattice, we have to define two effective couplings, k_a^{eff} and k_b^{eff}, to replace the initial values. In terms of these couplings we can calculate the dimensionless constants a^* and b^*, which describe the influence of the homogeneous lattice (with springs k_a^{eff} and k_b^{eff}) on bonds of type a and b. Once this is done, the effective medium reduces to the solution of the equations:

$$\frac{k_a^{\text{eff}}}{k_a} = \frac{p - a^*}{1 - a^*}, \tag{8a}$$

$$\frac{k_b^{\text{eff}}}{k_b} = \frac{p - b^*}{1 - b^*} \tag{8b}$$

with the additional constraint

$$a^* + 2b^* = 2. \tag{9}$$

Both a^* and b^* are functions of $k_a^{\text{eff}}/k_b^{\text{eff}}$ that can be calculated from the dynamical matrix of the reconstructed triangular lattice. Inserting (9) into (8), and dividing, we obtain

$$\frac{k_a^{\text{eff}}}{k_b^{\text{eff}}} = \frac{k_a}{k_b}\frac{a^*(p - a^*)}{(1 - a^*)(2p - 2 - a^*)}, \tag{10}$$

where we also have

$$a^* = a^*\left(\frac{k_a^{\text{eff}}}{k_b^{\text{eff}}}\right) \tag{11}$$

and

$$a^*(0) = 0,$$

$$a^*(1) = \tfrac{2}{3}, \tag{12}$$

$$a^*(\infty) = 1.$$

The general features of the solution of these equations can be inferred from the graphical representation of the function defined in Eq. (11). This is done in Fig. 3. The percolation threshold, determined by $k_a^{\text{eff}}/k_b^{\text{eff}} = 1$,

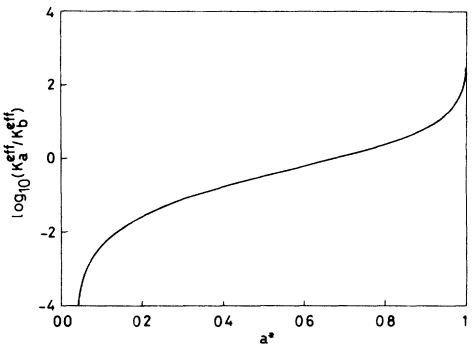

FIG. 3. Plot of the effective medium relation of Eq. (11). See the text.

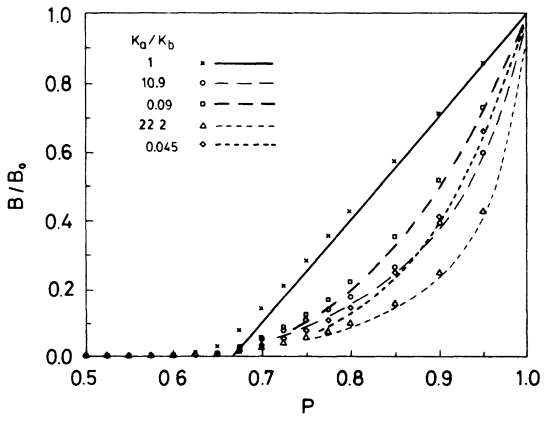

FIG. 4. Effective medium (lines) and numerical results for the bulk modulus vs p (discrete values). Results for different values of k_a/k_b are shown. The side of the hexagons in the simulations is 24.

is found to occur at $p_{cen} = \frac{2}{3}$,[16] which can also be obtained by counting the number of constraints.[11] This result is independent of λ_0/μ_0. Moreover, the ratio of the elastic moduli of the percolating network is such that $\lambda^{eff}/\mu^{eff} = 1$ at p_{cen}, in agreement with arguments based on other models,[3,4] and also numerical simulations[4] (see the following).

Close to $p = 1$ we can linearize Eq. (8) and obtain

$$k_a^{eff} = k_a \left(1 - \frac{1-p}{1-a^*(k_a/k_b)}\right),$$
$$k_b^{eff} = k_b \left(1 - \frac{2(1-p)}{a^*(k_a/k_b)}\right). \tag{13}$$

An explicit expression for the bulk modulus can also be obtained:

$$\frac{B}{B_0} = 1 - (1-p)\frac{a^*(k_a/k_b - 4) + 4}{(1-a^*)a^*(k_a/k_b + 2)}. \tag{14}$$

When comparing these equations to the continuum approximation [Eq. (7)], it is worth remembering that both k_a/k_b and k_b/k_a correspond to the same value of λ_0/μ_0. Thus, Eq. (14) is not uniquely determined by the continuum properties of the lattice. This is an indication that, contrary to scalar percolation, discrete lattice effects change the qualitative features of the solution. We further note that the slope at $p = 1$ [see Eq. (14)] is larger for $k_a/k_b < 1$ than for $k_a/k_b > 1$; this can be easily checked for $k_a/k_b \sim 1$ by noting that around this value Eq. (11) takes the simple form $\log_{10}(k_a/k_b) \sim 3a^* - 2$.

A complete plot of the solutions of Eqs. (10) and (11) is given in Figs. 4–6 for various initial values of k_a/k_b. The results are in reasonable agreement with the numerical simulations (also shown in Figs. 4–6) over the entire range of values of p. The rate at which the macroscopic constants approach zero depends on the initial ratio of λ_0/μ_0, although not on the percolation threshold (p_{cen}) nor on the ratio λ/μ at p_{cen}. This can be more explicitly seen in several ways. First we look at the effective-medium-theory results. Near the threshold ($p_{cen} = \frac{2}{3}$) the elastic moduli take the form

$$B \sim 6\mu_0(p - p_{cen}),$$
$$\mu \sim 3\mu_0(p - p_{cen}), \tag{15}$$
$$\frac{B}{\mu} = 2.$$

These results are independent of the microscopic details of the model (ratio of k_a/k_b); moreover, the critical behavior of the moduli (typical of mean-field theories) is also independent of the initial values of the macroscopic elastic constants. On the other hand, the actual value of p_{cen} (Ref. 4), $\frac{2}{3}$, is close to the result of numerical simulations (~ 0.65) and independent of both the macroscopic properties of the media (λ_0 and μ_0) and of the microscopic details of the model (k_a and k_b). As regards the numerical results, we note that they also indicate that the threshold occurs near $\frac{2}{3}$, and that, at this point, $\lambda/\mu \sim 1$, both results being independent of k_a/k_b. To make this point stronger, and, as finite-size scaling[17] cannot be performed within the present approach without excessive numerical errors (see the following), we have calculated the bulk modulus for a very large value of k_a/k_b (50); the results are shown in Fig. 7. We note that B approaches zero at a value of p very similar to that corresponding to $k_a/k_b = 1$, supporting the preceding conclusions. It is worth remarking that the actual behavior of B is very well approximated by Eq. (7) when $k_a/k_b = 1$ ($\lambda_0 = \mu_0$) up to very near the percolation transition (see Fig. 7), whereas, when $k_a/k_b \neq 1$, spatial correlations seem to become more important and the two curves deviate appreciably even far from p_{cen}.

These results are in agreement with continuum models that indicate that the critical properties of elastic percolation are independent of the macroscopic properties of the system, and also with rigorous arguments[8] that demonstrate that the percolation threshold for discrete models with only nearest-neighbor central forces should always be at the same value (whatever reconstruction of the lattice is chosen).

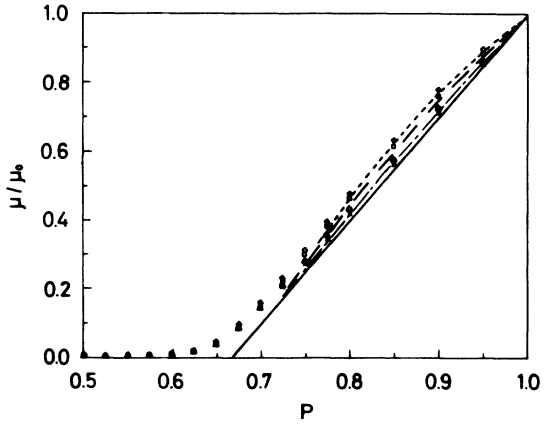

FIG. 5. Same as Fig. 4 for the shear modulus.

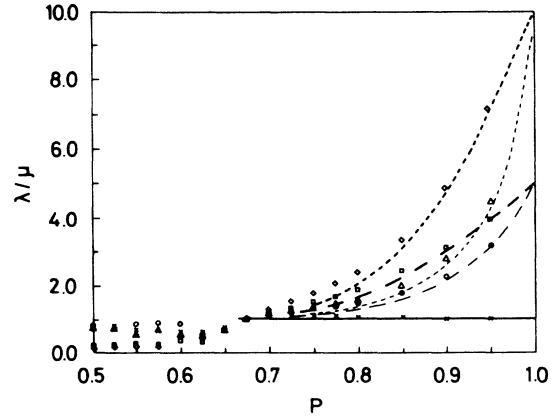

FIG. 6. Same as Fig. 4 for λ/μ.

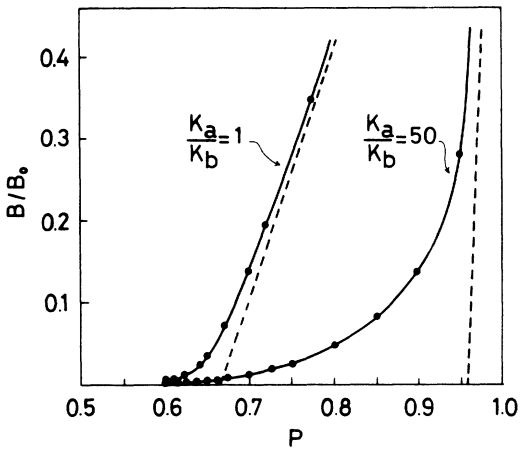

FIG. 7. Normalized bulk modulus as a function of p. Dots represent the results of our numerical simulations for a hexagon of side 48 [continuous lines are drawn as a guide to the eye, and dashed lines correspond to the approximation of Eq. (7)]. Two different values of k_a/k_b, 1 and 50 are shown.

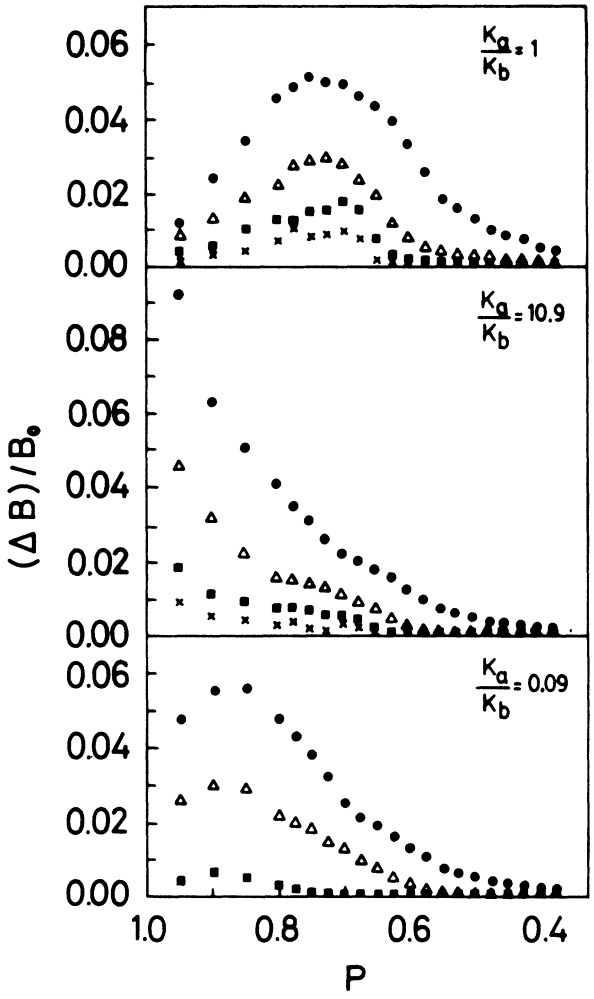

FIG. 8. Deviations of the bulk modulus ($\Delta B/B_0$) vs p for different values of k_a/k_b. Results for several sizes of the hexagonal samples are shown: • hexagon side 6, △ 12, □ 24, and × 48.

C. Mean deviations in the bulk modulus

We have also calculated the mean deviation in the bulk modulus ($\Delta B/B_0$) as a function of sample size for different values of p and λ_0/μ_0. The results are shown in Fig. 8. For $\lambda_0/\mu_0 = 1$ (unreconstructed triangular lattice), this function has a maximum near $p_{\rm cen}$, in agreement with the intuitive expectation that fluctuations should be most important near $p_{\rm cen}$. When the two types of springs are very different, a second peak develops at smaller concentrations of broken bonds. This peak approaches the point $p = 1$ as the ratio k_a/k_b is either zero or infinity (note that $\Delta B/B_0$ is always zero for $p = 1$). This effect is due to the fact that, when the bonds are very different, the elastic properties of the lattice are strongly dependent on the ratio of the bonds that are missing, which can deviate from the average value 2. As expected, the values of $\Delta B/B_0$ decrease with increasing sample size, as these deviations diminish. However, this anomalous peak in $\Delta B/B_0$ for intermediate sample sizes makes a finite-size scaling analysis of the elastic properties difficult. Spurious crossings in the graphs of $\ln[B(L)/B(L')]/\ln(L/L')$ versus p may appear, which was one of the reasons for the erroneous conclusion that $p_{\rm cen}$ depended on λ_0/μ_0.[7,8] This behavior of $\Delta B/B_0$ is also related with the finite-size effects and with the particular boundary conditions. The finite-size errors decrease considerably with increasing sample size, so it seems reasonable that finite-size scaling could be done confidently with larger system sizes in future works. Also the transfer-matrix approach could be done to determine more exactly the percolation threshold and the exponents. In this case, care should be taken because the boundary conditions do not generate a uniform dilation but rather uniaxial stresses, which could have some implications in the isotropy of the results.

D. Distribution of stresses

A similar effect can be observed in the distribution of stresses among the bonds of the lattice, as shown in Fig. 9. When all the springs have the same force constant this

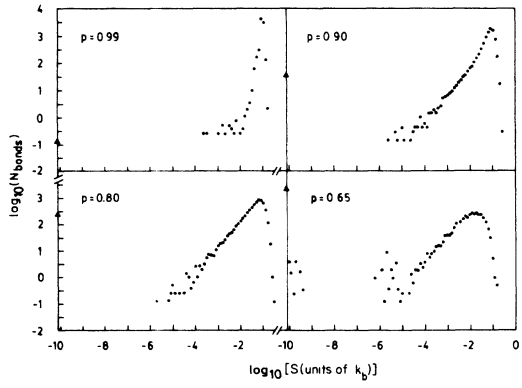

FIG. 9. Stress S (units of k_b) distribution in logarithmic scale. Results for an hexagon of side 30 and $k_a/k_b = 1$.

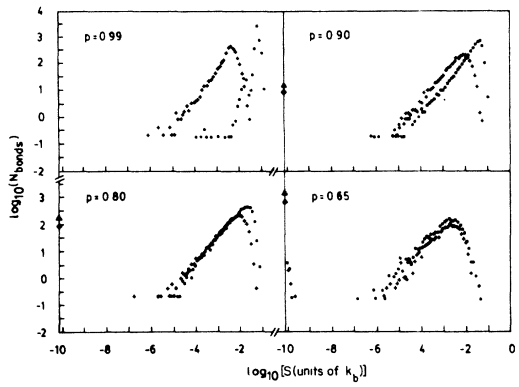

FIG. 10. Same as Fig. 9 for $k_a/k_b = 0.05$; • hard bonds and + soft bonds; △ hard bonds with stress less than 10^{-10} and ◇ soft bonds with stress less than 10^{-10}.

distribution has a pronounced maximum near $p = 1$. As the percolation threshold is approached, stresses become evenly distributed, signaling, as before, an increasing importance of fluctuations near the critical point. When the two types of bonds are very different (Fig. 10), close to $p = 1$, the stress distribution has two peaks for the backbone, reflecting the fact that, for homogeneous strains, the two bonds store different stresses. As the concentration of broken bonds is increased, this doubly peaked structure dissappears, which suggest that the stresses, and not the strains, are more homogeneously distributed. The values at which this crossover takes place correlate with the maximum in $\Delta B/B_0$ discussed before. Thus, for values of λ_0/μ_0 very different from one, we can define a region of concentrations for which fluctuations are very important and where the elastic behavior of the lattice resembles that near the percolation threshold.

These anomalous features, which are closely associated with the microscopic details of the lattice, suggest that, unlike scalar percolation, elastic percolation most likely does not show a universal behavior[18] valid for different systems with the same long-range properties.

V. CONCLUDING REMARKS

In this work we have investigated the properties of two-dimensional percolating networks in a model description of isotropic elastic media that combines a central-force Hamiltonian with a reconstructed triangular lattice (two different spring constants, k_a and k_b, where needed); the model allowed us to vary the ratio between Lamé coefficients from unity to infinity. We have analyzed the behavior of diluted networks away from and near to the percolation threshold by means of an effective-medium theory and numerical simulations. We think that we have presented conclusive evidence indicating that, contrary to previous results,[7] the percolation threshold is neither dependent on the macroscopic elastic properties of the system (λ_0 and μ_0) nor on the microscopic details of the model.[8] Moreover, at $p_{\rm cen}$, λ/μ also has the same degree of universality, being equal to unity. Instead, away from the percolation transition, our results suggest that the behavior of diluted elastic networks might strongly depend on how the voids are distributed. For concentrated voids the elastic properties are uniquely determined by λ_0 and μ_0. On the other hand, in the case of randomly distributed voids (percolating networks) the elastic properties also depend on the microscopic details (k_a and k_b) of the model used to describe the elastic medium with coefficients λ_0 and μ_0. Thus, we may conclude that elastic percolation does not seem to have the same degree of universality as scalar percolation.[18]

ACKNOWLEDGMENTS

We wish to acknowledge financial support from the Comisión Interministerial de Ciencia y Technologia (Project No. PB85-0437-C02), and one of us (O.P.) wishes to acknowledge a grant from Ministerio de Educacion y Ciencia. Also we thank H. Herrmann for helpful conversations.

[1] D. J. Bergman and Y. Kantor, Phys. Rev. Lett. **53**, 511 (1984)
[2] J. G. Zabolitzky, D. J. Bergman, and D. Stauffer, J. Stat. Phys. **44**, 211 (1986)
[3] Y. Kantor and I. Webman, Phys. Rev. Lett. **52**, 1891 (1984).
[4] L. M. Schwartz, S. Feng, M. F. Thorpe, and P. N. Sen, Phys. Rev. B **32**, 4607 (1985).
[5] *Percolation Structure and Processes*, Vol. 5 of *Annals of the Israel Physical Society*, edited by G. Deutscher, R. Zallen, and Joan Adler (Hilger, Bristol, 1983).
[6] S. Roux and A. Hansen, Europhys. Lett. **6**, 301 (1988); A. Hansen and S. Roux, Phys. Rev. B **40**, 749 (1989).
[7] R. Garcia-Molina, F. Guinea, and E. Louis, Phys. Rev. Lett. **60**, 124 (1988). See also comments to this paper in Ref. 8.
[8] S. Tyc, Phys. Rev. Lett. **61**, 2500 (1988); S. Roux, A. Hansen, and E. Guyon, *ibid.* **61**, 2501 (1988); A.R. Day and M.F. Thorpe, *ibid.* **61**, 2502 (1988); R. Garcia-Molina, F. Guinea, and E. Louis, *ibid.* **61**, 2503 (1988).
[9] L. D. Landau and E. M. Lifshitz, *Theory of Elasticity* (Pergamon, New York, 1959).
[10] M. A. Lemieux, P. Breton, and A.-M. S. Tremblay, J. Phys. (Paris) Lett. **46**, L1 (1985); A. R. Day, R. R. Tremblay, and A. M. S. Tremblay, Phys. Rev. Lett. **56**, 2501 (1986).
[11] S. Feng, M. F. Thorpe, and E. Garbozci, Phys. Rev. B **31**, 276 (1985); S. Feng, B. I. Halperin, and P. N. Sen, *ibid.* **35**, 197 (1987).
[12] E. J. Garbozci and M. F. Thorpe, Phys. Rev. B **31**, 7276 (1985).
[13] Note that this expression is different from that given in the original paper (Ref. 7). We thank E.J. Garbozci for calling our attention to this point.
[14] S. Feng and P. N. Sen, Phys. Rev. Lett. **52**, 216 (1984).

[15]M. F. Thorpe and P. N. Sen, J. Acoust. Soc. Am. **77**, 1674 (1985).
[16]This result coincides with that derived within effective medium theories; see, for instance, Ref. 13.
[17]M. Sahimi and J. D. Goddard, Phys. Rev. B **32**, 1869 (1985).
[18]S. Arbabi and M. Sahimi, J. Phys. A **21**, L863 (1988); M. Sahimi and S. Arbabi, Phys. Rev. B **40**, 4975 (1989).